Journal of Engineering and Sustainable Development
Vol. 30, No. 01, January 2026
https://jeasd.uomustansiriyah.edu.iq/index.php/jeasd
ISSN 2520-0917
Research Article
https://doi.org/10.31272/jeasd.3112

Baffle Pier Effects on Hydraulic Performance and Scour Downstream of Sluice Gates

Ibrahim M.M[1], Baydaa Hamdi Salih[2], Ahmed M. Ibraheem[3], Abeer Samy[1*]

[1] Civil Engineering Department, Shoubra Faculty of Engineering, Benha University, Cairo, Egypt
[2] Civil Engineering Department, Faculty of Engineering, University of Anbar, Ramadi, Iraq
[3] National Water Research Center, Hydraulics Research Institute, Qalyubia, Egypt

[*]Email: abeer.samy@feng.bu.edu.eg

Article Info

Received	03/11/2024
Revised	02/10/2025
Accepted	04/10/2025

Abstract

Sluice gates control water levels and discharge them into small irrigation canals. This study examined a modified stilling basin incorporating submerged baffle piers downstream. The study analyzed hydraulic-jump characteristics, energy-dissipation efficiency, velocity distribution patterns, water-level fluctuations, and bed configurations resulting from flow downstream of the sluice gate. The experimental program comprised ninety runs using ten stilling basin models. These models involve various stilling basins with different baffle pier heights and angles, tested under a range of flow conditions. A smooth apron without baffle piers served as the reference case for comparison. Results showed that baffle piers with a height of 12 cm and a 45° angle oriented against the flow optimized stilling basin performance, improving flow characteristics and minimizing bed configuration. This optimal design decreased dimensionless jump length by 45-47%, increased energy dissipation efficiency by 46-60%, and reduced maximum velocity by 33% compared to the smooth apron across the tested Froude number range. Based on these results, a multiple regression analysis was conducted to develop an empirical equation to predict energy dissipation in the modified stilling basins. These findings provide practical design guidelines for optimizing the performance of stilling basins in small irrigation canal systems.

Keywords: Baffle piers, Energy Dissipation, Flume, Hydraulic jump, Stilling Basin, Scour, Silting.

1. Introduction

Installing hydraulic structures to regulate water levels in waterways typically causes downstream turbulence via hydraulic jumps. This turbulence develops different bed configurations, including scour holes and sedimentation regions. Many trials have been applied to minimize turbulence, mainly by installing stilling basins downstream. Previous studies proved that installing obstacles on the apron downstream of sluice gates increases bottom friction. This increased friction decreases jump characteristics and local scour holes by reducing energy losses.

Both numerical and experimental models were employed to enhance the efficiency of downstream hydraulic structures. Several researchers have focused on the role of baffle blocks and stilling basins. For instance, Aydin and Ulu [1] used Computational Fluid Dynamics (CFD) to study the effect of different types of baffle blocks placed on a stilling basin downstream of an ogee weir. The performance of the modeled geometries was evaluated based on flow characteristics and downstream bed morphological changes in stilling basins. They reported that triangular baffle blocks with vertical upstream faces were the most effective. Also, using baffle blocks with a sill reduced the scour from 80% to 90%. Rdhaiwi et al. [2] applied research on the C-type trapezoidal piano key weir. They demonstrated that incorporating a stilling basin significantly reduced the maximum scour depth by 63.4% relative to configurations without a basin. The stilling basin altered the morphology of the scour hole, creating a more elongated profile and increasing the distance between the weir toe and the maximum scour location by 20.4%. The flow conditions, particularly the discharge rates, and the tailwater depths were identified as critical parameters influencing scour development, emphasizing the importance of these factors in the hydraulic structure design. Building on this, Fatima et al. [3] conducted CFD analysis of a USBR Type III stilling basin. They found that increasing wall convergence angles by up to 2.5° significantly improved energy dissipation by up to 14.5%,

whereas modifying impact blocks yielded an additional 2% improvement. They maintained stable post-jump Froude numbers between 0.6 and 0.78, demonstrating optimal performance when combining 2.5° wall convergence with modified friction blocks. These findings provide valuable design parameters for enhancing the efficiency of stilling basins through geometric modifications. Abdelmonem et al. [4] experimentally studied the effect of using a pendulum sill downstream of the sluice gate. A cylindrical steel sill with a constant diameter of 3 cm was used. The location of the pendulum sill, the discharge flow, and the gate opening were varied during the experimental work. The experimental results showed that the optimum location of the pendulum sill was in the first half of the hydraulic jump. Ashour et al. [5] conducted a physical study to investigate untested geometries of curved dissipaters with 21 different angles of curvature and arrangements. The tested shapes are evaluated by assessing their efficiency in dissipating the kinetic energy of water. Generally, the results showed that the dissipators were more effective at dissipating energy when the curvature was opposite to the flow direction. Also, the energy loss ratio increased with the increase of the curvature angle (θ), up to (θ= 120°), then it decreased again. Abdel Samad et al. [6] conducted an experimental study using a semi-circular sill with various heights and positions under different flow conditions. The case of a flat floor without a sill was also examined as a reference. The influence of the semi-circular sill on the dimensions of the scour hole is evaluated. The study found that using a single line of semi-circular sill yielded the most significant reduction in scour geometry, ranging from 71% to 88%, under the operating flow conditions. Fošumpaur et al. [7] presented experiments to describe the boundary condition for designing new fiber concrete dissipators based on the measurements performed on reinforced block ramps. The study concluded that the fiber concrete significantly improved the resistance of the reinforced block ramps.

Daneshfaraz et al. [8] investigated the effect of screens as energy dissipators. The experiments were conducted using screens with porosities of 40% and 50%, as well as single- and double-screen arrangements. The tested supercritical Froude numbers ranged between 5 and 18. The results outlined that using double screens with 40% porosity has the highest energy dissipation. Additionally, single screens with 50% porosity exhibit the minimum bed scour for a constant level of energy dissipation. Abbas et al. [9] studied experimentally the effect of different shapes of baffle blocks installed on stilling basins at adverse and horizontal slopes on the characteristics of the hydraulic jump. The experiments were conducted for initial Froude numbers (Fr1) ranging from 3.99 to 7.48. The study concluded that using a baffle block reduced the sequent depth ratio, jump length, and roller length, and increased the energy dissipation ratio. Elnikhely [10] studied experimentally the effect of cylindrical blocks with different diameters, lengths, and arrangements fixed on the back slope of the spillway on the scour hole parameters downstream of the spillway. The results identified the optimal block arrangement and dimensions that reduced relative scour depth by 34.2%. Ibrahim [11] experimentally tested oriented vanes on stilling basins to reduce scour and silting downstream of sluice gates. Using various configurations and flow conditions ,a formula has been developed to predict the erosion patterns. Dashtban et al. [12] found that baffle blocks in circular stilling basins enhance hydraulic jump stability and performance. The experimental results show that increased obstruction and subsequent radius ratios significantly influence jump characteristics. The study established that circular hydraulic jumps are considerably shorter than classical jumps and derived validated relationships for predicting the sequent depth ratio and energy loss. These findings provide practical design guidelines for implementing baffle blocks in circular stilling basins to optimize hydraulic jump behavior.

Aamir et al. [13] applied experimental research. The results showed that roughened stiff aprons can reduce maximum scour depth by 70-83% compared to smooth aprons, primarily due to the increased decay rate of submerged wall jets. The study established that scour depth decreased with larger sediment size, sluice opening, and apron length, whereas Froude number increased. Tailwater depth showed a distinctive U-shaped relationship with scour depth. An empirical equation incorporating apron roughness effects was developed to accurately predict maximum scour depth, addressing a significant gap in existing predictive models. Using a validated numerical model. Hojjati and Zarrati [14] demonstrated that scour hole profiles downstream of stilling basins are significantly influenced by Froude number and bed material size, while establishing that the upstream profile of the scour hole can be expressed through dimensionless parameters independent of time and material size. The study revealed that oscillating hydraulic jumps produce longer scour holes than steady jumps, providing crucial insights into the relationship between flow conditions and scouring patterns. The research developed a practical method for calculating long-term maximum scour depth across various hydraulic parameters through comprehensive numerical and experimental analyses, providing a valuable tool for engineering applications in stilling basin design.

Helal [15] conducted experimental studies to investigate the effect of a single line of floor water jets on scour-hole parameters downstream of a Fayoum-type weir. The outcomes demonstrated that using a single row of floor jets at 40% of apron length reduced the maximum scour depth by 90% compared to the floor without water jets. Amin [16] conducted a physical study to investigate the effect of using double lines of floor water jets with different downstream spillway arrangements. The results indicated that the maximum reductions in scour depth ranged from 5% to 68%, and in scour length from 49% to 76%. Helal et al. [17] numerically studied the performance of five lines of floor jets with different jet flow discharges in submerged hydraulic jumps. Computational fluid dynamics (CFD) modeling was used to simulate the submerged-jump characteristics. The outcomes showed that the bed water jets increased the efficiency of the submerged hydraulic jumps by up to 85.4% and reduced the submerged jump length by up to 59% relative to the non-jetted system. Erryanto and Dermawan [18] investigated double sills in stilling basins for roller-compacted concrete (RCC) gravity dams as an innovative energy-dissipation solution, with the Froude number at the spillway toe determining hydraulic-jump

behavior. Hydraulic modeling demonstrates the effectiveness of double sills in reducing the flow energy and maintaining subcritical conditions downstream of steep chutes. The research provided practical design insights to enhance stilling basin performance and prevent scour downstream of RCC dam structures. Saleh et al. [19] conducted experimental and numerical studies to optimize the dimensions and geometry of a labyrinth weir, employing it to minimize adverse hydraulic effects over weirs. The outcomes indicated that the labyrinth weir with a 60° crested angle increased the energy dissipation. Tuna and Emiroglu [20] experimentally studied the scour parameters downstream of cascades. Three different flow regimes are examined. The findings indicated that the flow type on the stepped chutes was a significant factor in the formation of scour holes. Lower scour depths are observed in the nappe flow regime than in the transition and skimming flow regimes. Also, the measured velocity at the end of the stilling basin increased with the chute channel base angle.

Al-Husseini et al. [21] studied the effect of upstream sluicegate and chutes in a stepped cascade weir on energy dissipation experimentally. Muhsun et al. [22] employed both experimental and numerical models to identify an appropriate crest depth position for estimating the flow rate over a curved Crump weir under ten different slope conditions. The estimated flow rates were subsequently compared with measured data and those obtained from Computational Fluid Dynamics (CFD) simulations. Al-Husseini et al. [23] used an experimental and numerical model to study the scour downstream of a sharp-crested weir. The research concluded that the optimal design is inclined weirs with a 120° angle to mitigate scour around hydraulic structures.

While previous studies have investigated various energy dissipation methods, a comprehensive analysis of how the height and orientation angle of submerged baffle piers interact to affect hydraulic performance was still lacking. Therefore, the present study aimed to address this gap by experimentally investigating the effects of systematically varied baffle-pier geometries on energy dissipation, velocity distribution, and downstream bed configuration. The objective was to identify an optimal pier arrangement for maximizing stilling basin efficiency.

2. Dimensional Analysis

A large number of flow and sediment variables were considered in the investigations of the flow pattern, the flow characteristics, and the local bed configurations downstream of the sluice gate with a stilling basin equipped with baffle piers fixed on its surface; these parameters were listed as follows:

The flume width, B; the stilling basin length, L_f; the gravity acceleration, g; the flume bed slope, S_o; the baffle pier height, P_h; the baffle pier width, P_w; the baffle pier distance from the sluice gate, P_d; the baffle pier angle with respect to flow direction, P_θ; the median particle diameter, d_{50}; the flow discharge, Q; the tailwater depth, y_t; the gate opening height, y_g; the upstream water head, H_{up}; the water dynamic viscosity, μ; the water density of the flow, ρ; the water surface tension, σ; the soil particle density, ρ_s; the energy dissipation efficiency, η; the hydraulic jump initial flow depth, y_1; the hydraulic jump sequent flow depth, y_2; the hydraulic jump length, L_j; the mean longitudinal velocity, V; the hydraulic jump initial velocity, V_1; the hydraulic jump sequent velocity, V_2; the maximum velocity at any cross section downstream the apron, V_m; the maximum scour depth, d_s; the maximum scour length, L_s; the longitudinal distance measured from the apron toe to a given location along the flume, X.

$$\eta = \frac{E_2}{E_1} \qquad (1)$$

Where E_1 and E_2 are the initial and sequent specific energies, respectively.

$$E_1 = y_1 + \frac{V_1^2}{2g} \qquad (2)$$

$$E_2 = y_2 + \frac{V_2^2}{2g} \qquad (3)$$

$$f\begin{pmatrix} B, H_{up}, L_f, g, V, V_1, V_2, V_m, L_j, S_o, y_t, y_1, y_2, Q, y_g, \\ P_h, P_w, P_d, P_\theta, d_{50}, d_s, L_s, \rho, \mu, \sigma, \rho_s, \eta, X \end{pmatrix} = 0 \qquad (4)$$

In this study, B, H_{up}, L_f, ρ, S_o, d_{50}, P_w, and P_d are kept constant throughout the experimental program. Therefore, they are neglected in (4). The balanced time for scouring and silting geometries was fixed for all experiments. Using π-theorem and applying the properties of dimensional analysis, it yields;

$$f\left(\frac{P_h}{y_t}, P_\theta, \frac{X}{y_2}, \eta, \frac{V}{\sqrt{gy}}, \frac{\rho Q}{B\mu}, \frac{\rho V^2 B}{\sigma}, \frac{d_s}{y_t}, \frac{L_s}{y_t}, \frac{L_j}{y_1}, \frac{L_j}{y_2}\right) = 0 \qquad (5)$$

But $\frac{V}{\sqrt{gy}}$ is the Froude number, F_r; and $\frac{\rho Q}{B\mu}$ is the Reynolds number, R_e, and $\frac{\rho V^2 B}{\sigma}$ is the Weber number.

Using π-theorem and applying the properties of dimensional analysis, it yields;

$$f\begin{pmatrix} \frac{P_h}{y_t}, P_\theta, \frac{X}{y_2}, \eta, F_r = \frac{V}{\sqrt{gy}}, R_e = \frac{\rho Q}{B\mu}, \\ W_e = \frac{\rho V^2 B}{\sigma}, \frac{d_s}{y_t}, \frac{L_s}{y_t}, \frac{L_j}{y_1}, \frac{L_j}{y_2} \end{pmatrix} = 0 \qquad (6)$$

The effects of viscosity and surface tension are assumed to be secondary, since the flow is primarily gravitational in an open channel. Therefore, the impact of Reynolds and Weber numbers, R_e and W_e, can be neglected. Hence, (6) may be written in the following form:

$$f\left(\frac{P_h}{y_t}, P_\theta, \frac{X}{y_2}, \eta, F_r, \frac{d_s}{y_t}, \frac{L_s}{y_t}, \frac{L_j}{y_1}, \frac{L_j}{y_2}\right) = 0 \qquad (7)$$

Clarifying (7), a distinction must be made between the independent and dependent variables in this dimensionless functional relationship. The independent variables are P_h, P_θ, y_t, and x. These parameters constitute controllable experimental conditions that were systematically varied throughout our investigation. Conversely, the dependent variables are L_j, y_1, y_2, F_r, d_s, and L_s. These parameters respond to changes in independent variables and characterize the resulting hydraulic performance and bed morphology. The dimensionless groupings in (7) were derived using the Buckingham π theorem to maintain dimensional homogeneity and to represent the fundamental physical relationships governing flow and scour

phenomena downstream of sluice gates with baffle-pier stilling basins.

3. Methods and Materials

The experimental runs have been conducted in the laboratory flume at the Hydraulics Research Institute (HRI) of the National Water Research Center, Egypt. The flume has a length of 24.5 m, a width of 0.74 m, and a depth of 0.7 m. The flume depth increased to 0.95 m in the region where the bed material is located. The water feeds the flume through a recirculating system using a centrifugal pump that supplies water from the storage tank to the head tank. The head tank has a gravel box to ensure uniform flow distribution at the flume inlet. All parts of the flume, except the 2.25 m side walls, are constructed of bricks. The side walls are made of Plexiglass to allow visual observation and facilitate measurement of hydraulic jump characteristics. A gate valve is fitted on the main pipeline to control the flow rate supplied directly before the head tank. Fig. 1 shows a schematic of the flume used.

The downstream water depth was adjusted by a tilted steel tailgate installed at the flume end. The bed levels and water depths were measured with a point gauge and verified with a leveling device. The gauge was mounted on a moving carriage to cover the flume length and width. The sluice gate model was made of a steel plate 0.008m thick to prevent deformation under upstream water pressure. The sluice gate model had a width of 0.74 m and a height of 0.5 m. The downstream apron was 1.2 m long and 0.74 m wide, covering the flume width. To create the required roughness, 15 symmetrical steel baffle piers, each 0.1 m wide, were used. The baffle piers were arranged symmetrically in 5 rows and three columns to cover the middle 0.6 m of the apron. However, the first and last 0.3 m of the apron were flat without baffle piers; Fig. 2 shows the dimensions of the apron model used and the angles employed. The apron was followed by 0.25 m of bed material with median size d50 = 0.442 mm and bulk unit weight $\gamma b = 1.92$ g/cm^3. The gradation of the used bed material was characterized by the geometric standard deviation, $\sigma g = (d84/d16) = 0.5$; thus, $\sigma g = 2.06$. The bed material filled an area of 0.74 m in width and 2.0 m in length in the flow direction. The bed material was adjusted to be at the same level. Fig. 3 shows a schematic diagram of the flow pattern and bed configurations downstream of the sluice gate.

Many parameters were included in the experimental program; the ranges of the variables used are tabulated in Table 1.

3.1. Justifications of Parameters Assumptions

After several trials of the experimental work, the current study makes assumptions regarding the dimensions of the sluice gate model, the discharge, the tailwater depth, the baffle pier height, and the baffle pier angle of orientation. The parameter assumptions are:

- The sluice gate height was 0.50 m to allow freeboard for the flume to prevent water overtopping, considering the case of the tested maximum flow discharge; Q= 40 Lit/s.
- The minimum baffle pier height, P_h= 6 cm, because lower heights do not affect the flow pattern, especially for the case of minimum tested discharge; Q= 20 Lit/s. However, the maximum height of the baffle pier is P_h= 12 cm, as for longer P_h, the effect of air-water aeration is considered primarily for tests of discharge and tailwater depth of Q= 40 Lit/s and y_t= 18 cm, respectively.
- The baffle pier's angle of orientation P_θ ranged between 45 ° and 135 ° because the tested angles out of that range showed insignificant effect on bed configurations compared to the referenced case without baffle piers in the case of minimum tested flow conditions.
- The minimum operated tailwater depth, y_t= 18 cm, where lower values led to a complete movement for the bed material because of Q= 40 Lit/s due to the remarkable increase in the near-bed velocity. However, insignificant remarks in bed configurations are noticed for tested tailwater depths y_t higher than 24 cm, especially for Q= 20 L/s.

3.2. Experimental Program

The test program consisted of 90 experimental test runs, using ten different models (3 heights of the baffle pier with 3 angles, in addition to the model of smooth apron). Each model was operated under 3 flow discharges and 3 tailwater depths. To systematically investigate the impact of baffle pier configurations on flow characteristics and bed morphology, these ten distinct models were designed with a factorial approach. The first model served as the control case, featuring a smooth apron with no baffle piers (P_h=0 cm, P_θ= 0°). This baseline allowed for direct comparison with the modified designs. The other models explored a structured combination of baffle pier heights (P_h) and inclination angles (P_θ). Three different pier heights were tested (6 cm, 9 cm, and 12 cm), and for each height, three inclination angles were examined (45°-forward-leaning, 90°-vertical, and 135°-backward-leaning). This parametric design enabled a comprehensive assessment of how both the height and angle of baffle piers, individually and jointly, affect hydraulic jump characteristics, energy dissipation, scour patterns, and downstream sediment transport.

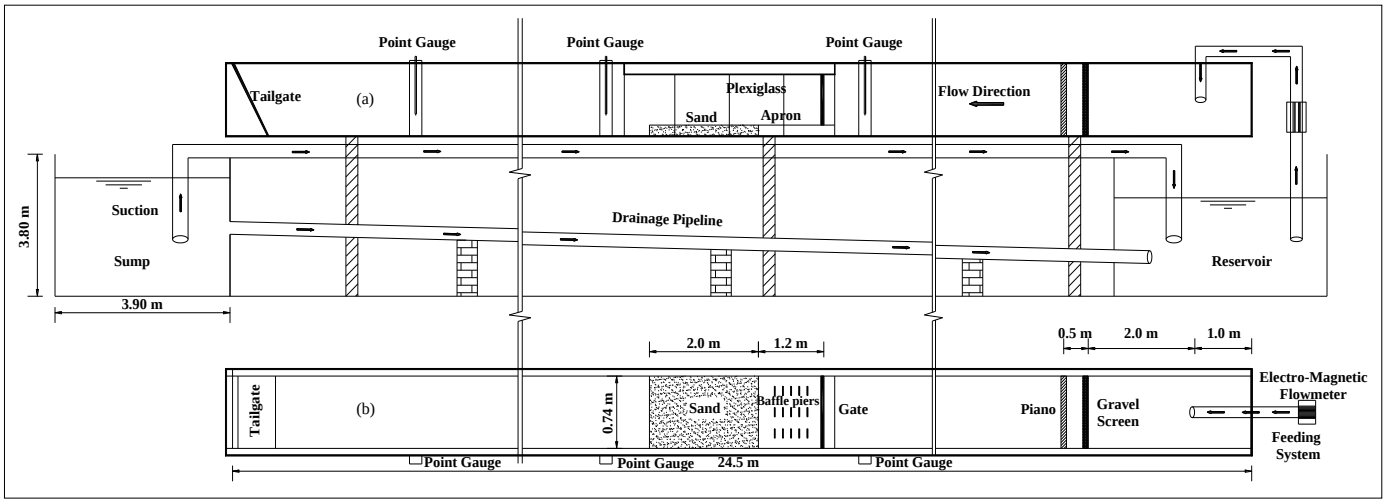

Figure 1. Definition sketch for the used flume: (a) elevation; (b) plan.

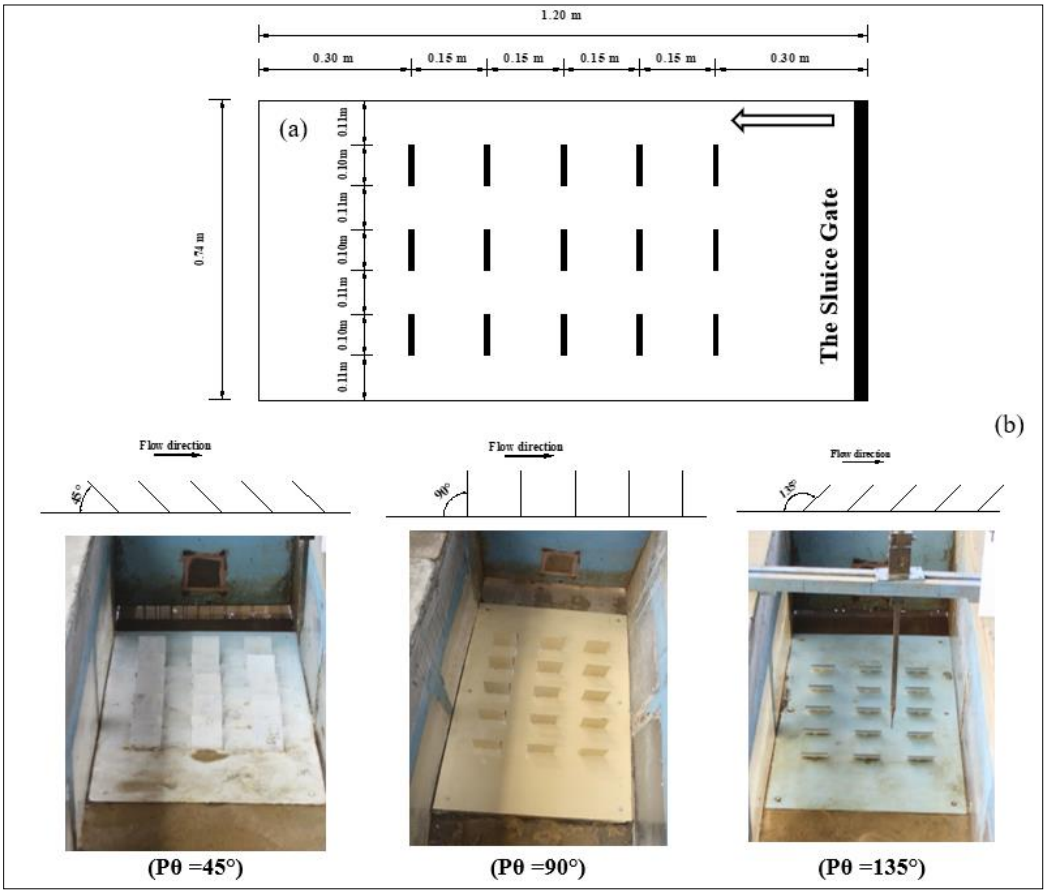

Figure 2. The used stilling basin: (a) dimensions; (b) baffle piers angles.

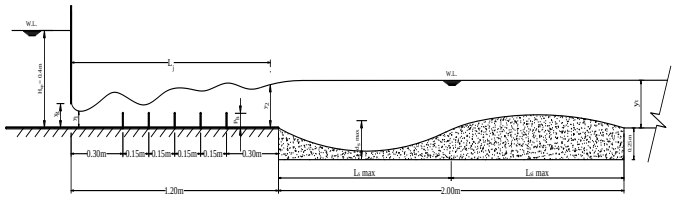

Figure 3. The schematic diagram for the flow pattern and bed configurations.

Table 1. The range of variables in the experiments

Parameter	Symbol	Value	Range		Unit
			From	To	
Discharge	Q	20, 30, 40	20	40	Lit/s
Baffle Pier Height	P_h	6, 9, 12	6	12	cm
Baffle pier angle of inclination	P_θ	0°, 45°, 90°, 135°	0°	135°	degree
Tailwater depth	y_t	18, 21, 24	18	24	cm
Gate opening height	y_g	1.6, 2.4, 3.1	1.6	3.1	cm

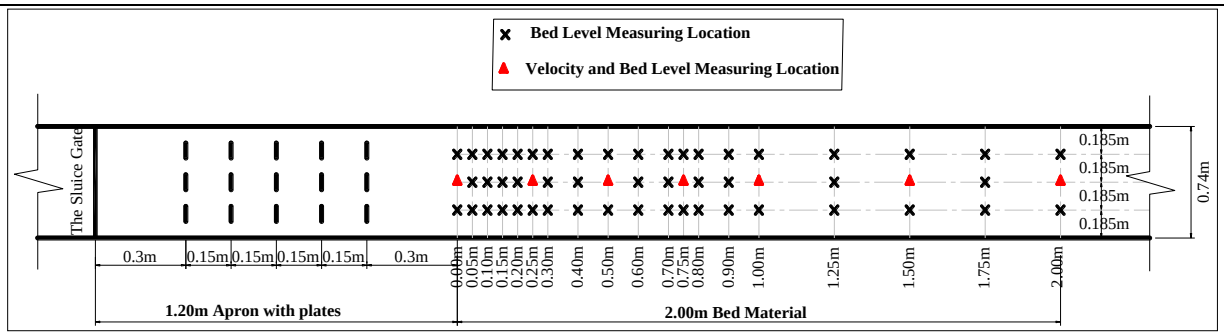

Figure 4. Locations of velocity and bed profile measuring points

To investigate the water-surface profile, water levels were recorded at 10 cm intervals along the mid-channel, starting just downstream of the sluice gate and extending to 2.0 m downstream of the stilling basin toe. The velocities were measured at 9 locations along the mid-channel, as shown in Fig. 4. At each location, the velocities were recorded at five vertical points: at 0.2, 0.4, 0.6, 0.8, and 0.9 of the measured water depth at that point. A mesh comprising 57 measurement points was used to provide a detailed description of the bed configurations. The locations of bed measurements were distributed into 19 sections along the flume length and three measuring points for each section, as shown in Fig. 4. The spacing between longitudinal sections was constant at 0.185 m. The spacing between sections was dense at the first 1 m of bed material, where the location of maximum local scour was predictable; thus, the bed profile was recorded at 45/57 measuring points. In the second 1 m of bed material, the spacing between sections increased to 0.25 m. Hence, only 12/57 points were used for bed profile measurements.

3.3. Run Procedure

To achieve the objectives of this study, the upstream water head was constant (H_{up}= 0.4 m). Three gate openings were used, y_g= 1.6, 2.4, and 3.1 cm, to convey the flow discharges (Q) = 20, 30, and 40 Lit/s, respectively. Ninety runs, including nine runs with a flat apron (without baffle piers), were used as a reference case in the comparison processes.

After filling the flume with the bed material fitted in place, it was accurately leveled to the apron level using a leveling device and checked with a point gauge, with an accuracy of ±0.1mm. For each test, the apron model was carefully installed in its designated position in the flume. The gate opening was adjusted using a Vernier caliper. The tailgate was closed, and backwater feeding was initiated until the water depth exceeded the required tailwater depth. Then, the upstream feeding started. The control valve on the main pipeline was gradually opened until the required discharge was measured with an ultrasonic flowmeter, with ±1% accuracy. The tailgate was progressively tilted until the required water depth was achieved, as indicated by the point gauge; thus, the test began. After 5 hours, when no changes in the bed profile were observed, the water-surface profile was recorded at 10 cm intervals, starting just downstream of the sluice gate and extending to the end of the bed-material area, 3.2 m downstream of the sluice gate, using a point gauge and an ordinary scale. The velocity measurements were recorded using an electromagnetic current meter (type E.M.S.) with an accuracy of ±0.2%. The main pump was turned off, and the tailgate was tilted very slowly to avoid affecting the bed configurations during flume drainage.

The bed levels were recorded at the location indicated in Fig. 4 using a Leica DNA-10 digital leveling device.

3.4. The Scale Effect

To emphasize the experimental scale effects, certain parameters were excluded from the experimental work because of their negligible influence, such as air aeration and cavitation, given the presence of baffle piers facing the high-velocity flow beneath the sluice gate. Additionally, because the flow is open-channel, the considered force is gravity; thus, surface tension and viscous forces, expressed in Weber and Reynolds numbers, may be ignored.

4. Results and Discussions

4.1. Flow Characteristics

To explore the influence of submerged baffle pier installation on the Froude number, taking into consideration the classical smooth apron, Fig. 5 was plotted. Froude numbers were estimated along the flume centerline in the bed-material region. The selected tested apron with baffle piers had P_h= 6 cm and P_θ= 90°. The figure was presented for hydraulic flow condition of Q= 40 Lit/s and y_t= 18 cm. In Fig. 5, notable differences in the Froude number were observed across the types of aprons employed. At the exact location of the bed material, with particular emphasis on the first half-length of the bed material, the installation of the baffle piers created obstacles facing the jet flow downstream of the sluice gate. Thus, most of the jump energy was dissipated, and the water turbulence decreased downstream of the apron. As a result, the flow velocity decreased; consequently, the Froude number decreased by 50.86% on average along the bed material for the apron with baffle piers compared to the smooth apron.

The figure also showed that the Froude number decreased with increasing bed material, regardless of the installed apron type. This was explained by the fact that the jump energy was partially dissipated in the region where the apron was installed. Part of this energy was conserved in the flow and gradually dissipated as the bed material was transported downstream. These findings were significantly highlighted for the smooth apron.

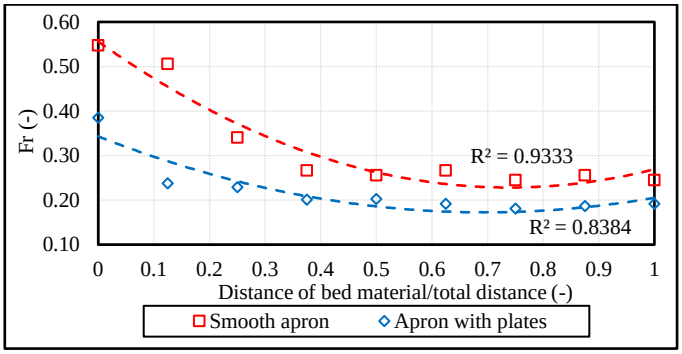

Figure 5. Froude number downstream aprons with and without baffle piers

4.1.1. The hydraulic jump characteristics

Measurements of water depth across the hydraulic jump were verified using several methods, with particular emphasis on the initial and subsequent depths. Firstly, by visual observation through the plexiglass flume side walls, where standard scales were fixed at 5 cm intervals, starting from the sluice gate and ending at the end of the bed material. The measurements of the ordinary scales were checked utilizing a leveling device. The sequent depth, y_2, was also calculated using (8), Fang. [24].

$$\frac{y_2}{y_1} = \frac{1}{2}[-1 + \sqrt{1 + 8Fr_1^2}] \quad (8)$$

The jump length was initially measured during the experiment by placing a steel rod with a thread at one end on the water surface. When the free end of the thread stopped moving, the location of the sequent depth was recorded and measured. The horizontal distance between the initial and subsequent depths was recorded as the jump length. Because of the inaccuracy and expected errors in measurements using the steel rod with a thread, a current meter was used to trace the positive and negative flow velocities. The horizontal distance between the location of zero velocity and the initial flow depth, y_1, was considered the hydraulic jump length.

To explore the influence of the baffle pier angles on the dimensionless hydraulic jump length, L_j/y_2 under different initial Froude numbers Fr_1; Fig. 6(a) was plotted for P_h= 6 cm, Q= 40 Lit/s, and y_t= 18 cm. It was found that the L_j/y_2 slightly increased with the increase of Fr_1 regardless of the tested angle. This was caused by the rise in the hydraulic jump initial velocity, V1, so Fr1 increased, and the water turbulence and the jump characteristics were accentuated.

For constant Fr_1, Fig. 6(a) illustrates that the L_j/y_2 decreased by employing an apron with baffle piers compared to a smooth apron. The installation of baffle piers increased apron friction, thereby dissipating more energy and reducing the jump characteristics. The figure demonstrates that an apron with a Pθ = 45 ° tilt angle has the shortest L_j/y_2 for a given Fr_1. This is reasoned by the 45 ° baffled piers that were pointed against the flow direction, which developed air-water aeration to improve the effectiveness of the used apron for the energy dissipation and, consequently, limiting the jump length. By contrast, the apron with a tilt angle of 135 ° showed the highest Lj/y2 among the angles tested. From a numerical perspective, the Lj/y2 decreased by 30.29%, 24.09%, and 11.91% on average for aprons with 45 °, 90 °, and 135 °, respectively, when considering the smooth apron.

Fig. 6(b) shows the influence of the baffle pier height, Ph, on the relative jump length L_j/y_2. The figure was presented for Q= 40 Lit/s, y_t= 18 cm, and P_θ = 45°. The selected angle was recommended for use because of its significant effect on Lj/y2, as discussed in Fig. 6(a).

Fig. 6(b) displayed that the higher baffle piers have a greater effect in decreasing Lj/y_2, where employing an apron with Ph= 12 cm effectively decreased the Lj/y_2 between 42.55% and 47.30% compared to the smooth apron. These outcomes, ascribed to the increase in baffle pier height, are attributable to the rise in the obstacle facing the turbulent flow, which dissipates more energy and consequently reduces the jump length.

Table 2 summarizes the influence of baffle piers installed on the smooth apron on jump characteristics. The table was provided for Ph = 12 cm, Q = 40 L/s, at different tailwater depths and baffle pier angles. The table confirmed Fig. 6(a) findings that baffled piers improved stilling basin efficiency regardless of tilt angle. The baffle pier of P_θ= 45° presented the optimum inclination angle where the maximum reductions in L_j/y_2 were recorded for the tested tailwater depths. Also, for constant P_θ, the baffle pier installation was slightly functional by increasing y_t.

Table 2. Effect of baffle piers angle on the relative Length of Jump Compared to the Smooth Apron.

Baffle piers angle y_t (cm)	%Reduction in L_j/y_2 for Q= 40 Lit/s, P_h=12 cm		
	P_θ =45°	P_θ =90°	P_θ =135°
18	45.39	39.23	27.02
21	45.50	39.97	27.89
24	47.25	40.75	28.54

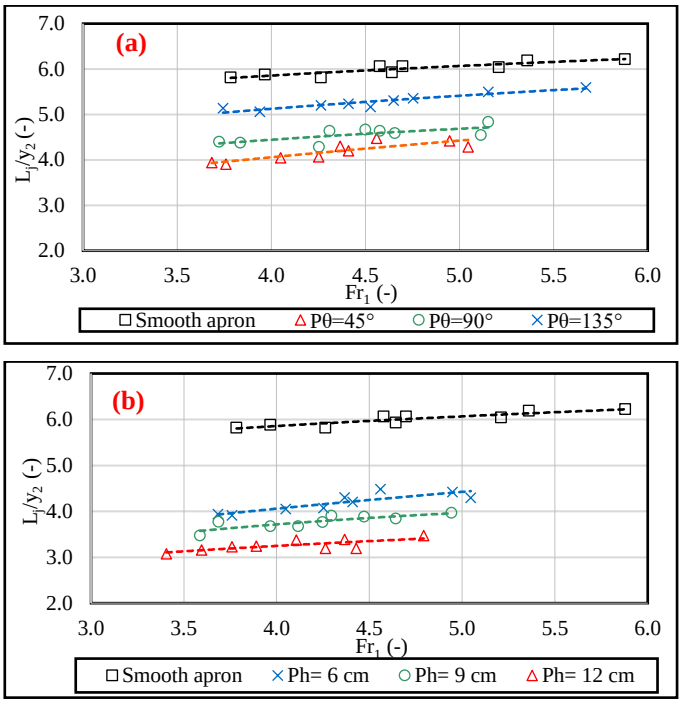

Figure 6. Dimensionless hydraulic jump lengths for baffle piers with different (a) angles; (b) heights.

4.1.2. The energy dissipation efficiency

Fig. 7 was plotted to assess the adequacy of the stilling basin with baffle piers in dissipating the jump energy. By applying dimensional analysis, the parameters listed in (7) can be used to study energy dissipation at the hydraulic jump. The relationship between the initial Froude number, Fr_1, and the energy dissipation efficiency, η, for different baffle-pier angles and heights was presented. Fig. 7 is plotted for Q = 40 L/s and y_t = 18 cm. The figure confirmed the findings discussed in subsection 4.1.1, in which installing a stilling basin with baffle piers, regardless of angle and height, effectively improved the flow characteristics of the hydraulic jump and increased the stilling basin efficiency. Fig. 7 demonstrated that the energy dissipation efficiency, η, was inversely proportional to the initial Froude number, Fr_1. To illustrate this, the findings from Fig. 6 may be employed: it concluded that Lj/y2 increased with Fr1, thereby decreasing the energy dissipation efficiency due to the installation of the stilling basin with baffle piers, as shown in Fig. 7.

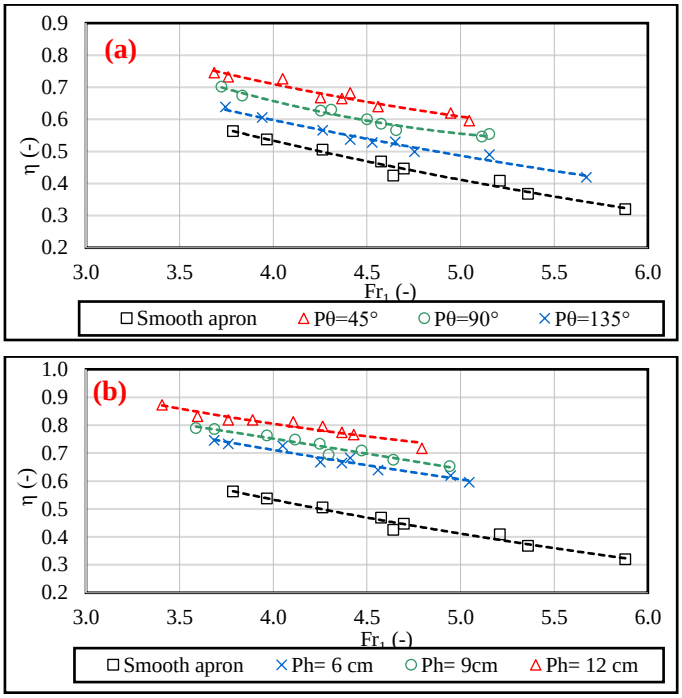

Figure 7. Energy dissipation efficiency for baffle piers with different (a) angles, (b) heights.

Fig. 7(a) is plotted for Ph = 6 cm, focusing on the influence of the baffle piers' angles, P_θ. The figure examined the superiority of baffle piers with Pθ = 45 ° compared with other tested angles. The figure indicates that the stilling basin with Pθ = 45 ° increased the energy dissipation efficiency, η, between 30.19% and 45.36%, for the same range of Fr1, when a smooth apron was used.

Regarding the baffle pier height, Ph, Fig. 7(b) shows that P_h significantly affects the energy dissipation efficiency, η. The figure is presented with Pθ = 45 °. The figure demonstrates that η increased with the increase of P_h for constant Fr_1, where the maximum η is achieved for P_h= 12 cm. Installing a baffle pier with P_h= 12 cm increased η between 45.64% and 59.55% compared to the smooth apron for the same range of Fr_1.

Based on the experimental data and employing the multi-regression analysis corresponding to the different flow conditions, several models, an empirical (9) for the energy dissipation efficiency, were developed and presented as follows:

$$\eta = \exp\left(0.577 * \left(\frac{P_h}{y_t}\right) - 0.0928 * P_\theta - 0.242 * Fr_1 + 0.482\right) \quad (9)$$

where: Coefficient of multiple determination (R^2) =0.8558, Standard Error of Estimate (SEE) = 0.0424, P_θ (in Radian).

4.1.3. The velocity distribution downstream of the apron

Fig. 8 shows the vertical-velocity distribution at the end of the stilling basin for Q = 40 L/s, yt = 18 cm, and Ph = 12 cm, considering different tested inclination angles, P_θ.

The figure shows that the mean velocity ratios, V/V1, decrease by 32.76%, 25.86%, and 6.90% for Pθ = 45 °, 90 °, and 135 °, respectively, compared with the smooth apron. Consequently, fixing baffle piers at Pθ = 45° on the apron yields the maximum

reduction in the velocity ratio V/V1, making it recommended from a velocity-distribution perspective. These findings are consistent with the discussions in the previous subsections 4.1.1 and 4.1.2.

For a thorough velocity investigation, Fig. 9 plots the velocity distribution at various locations along the flume length downstream of the stilling basin. The locations of measuring points were presented in Fig. 4. Fig. 9 showed that the influence of the baffle piers installation was significant at the first 0.5 m from the stilling basin toe, and then the effect of P_θ decreased along the flume length; X. Most of the flow turbulences reasoned to dissipation in the region of the stilling basin, where the baffle piers covered most of the jump length. The rest of these turbulences are extended longer distances than the stilling basin length, then gradually dissipated along the flume length, where the flow moved further than the stilling basin toe and was uniform again. At a given velocity-measuring location, the stilling basin with Pθ = 45 ° showed good performance in shifting the velocity distribution curve to lower values. For the tested models, flow velocities decreased through the seven sections downstream of the stilling basin toe, due to the development of a scouring hole in the bed material, which increased the flow depth. By the end of the scouring region, the flow velocities increased due to the decrease in flow depth, indicating the onset of the sedimentation zone. The complete study for the bed configurations was presented in section 4.2.

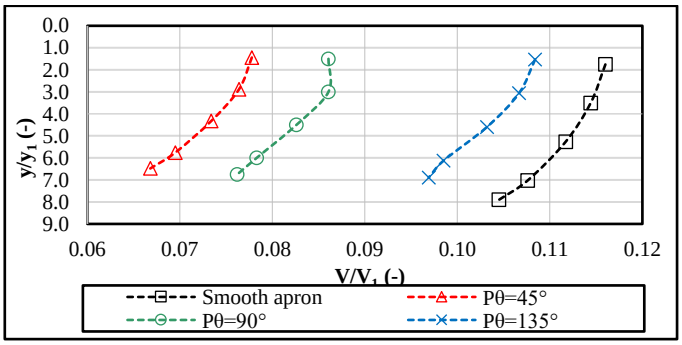

Figure 8. Vertical Velocity Distributions at the Stilling Basin Toe

Focusing on the effect of P_θ on the reduction of maximum velocity, V_m, taking into consideration the smooth apron at different locations along the flume length, X, Fig. 10 was plotted. The figure outcome was consistent with the findings in Fig. 9, which showed that the stilling basin with Pθ = 45 ° exhibited the most significant reduction in V_m at all recorded locations. On the other hand, Pθ = 135 ° recorded the minimum values. Consequently, it was recommended to use a stilling basin with Pθ = 45 ° to reduce the vertical-velocity distribution and the maximum velocities.

4.1.4. The water surface profiles

Water-surface profiles at different angles of baffle piers were obtained by recording longitudinal water levels for the other tested models. The observed measurements for the various tested scenarios are presented in Fig. 11. For Pθ, Fig. 11(a) shows that installing baffle piers in the stilling basin increased the water level due to a change in stilling basin friction. The changes in water levels were remarkable, beginning at the second row of baffle piers (i.e., at 0.45 m from the sluice gate) and ending at 1.4 m, where the flow became uniform, and jump action ceased.

By decreasing P_θ, the generated turbulences were maximized, and the water level was raised. Consequently, the velocity distribution and jump lengths decreased for constant Q, which agreed with the sub-sections 4.1.1, 4.1.2, and 4.1.3 conclusions.

Regarding the influence of discharge on water-level fluctuations in the presence of a stilling basin with baffle piers, Fig. 11(b) is shown. The figure shows that the initial jump depth, y1, is inversely proportional to Q. In contrast, the sequent depth, y_2, and the jump length, L_j, increased with Q. This indicates that as Q increased, the water passed through the sluice gate at a higher jet velocity, creating a longer region of water-level disturbance.

Finally, Fig. 11(c) emphasized the influence of y_t on the water surface profile. The figure demonstrated that increasing yt reduced the hydraulic jump characteristics. Because of the rise in y_t, the flow velocities under constant Q decreased, and accordingly, there was less disturbance in water levels, which limited the jump. The outcomes were consistent with those in Table 2.

4.2. Bed Configurations

The bed fluctuations were a motivating feature of the uniform sediment transport, which began to move once the drag and lift forces made the flow sufficient to overcome the frictional and gravitational forces that hold the grains in place. As sediment was transported or rolled into place, local scour occurred along the alluvial bed due to the flowing stream.

To investigate the influence of the baffle piers' angle on the bed configuration, Fig. 12(a) was plotted for a specific value of Q = 40 L/s, Ph = 6 cm, and yt = 18cm. The figure showed that the stilling basin equipped with baffle piers, regardless of their angles, reduced downstream local scour compared with the smooth apron. This was attributed to the remarkable energy dissipation resulting from the installation of baffle piers. Consequently, the minimum local scour geometry in terms of depth and length was recorded for Pθ = 45 °. This is explained by the baffle piers installation, which is oriented against the flow direction; Pθ = 45 ° increased the apron friction by presenting a repelling obstacle facing the flow, thereby generating turbulence to dissipate most of the jump energy. Thus, shorter hydraulic jump lengths, greater dissipation of jump energy, and lower longitudinal velocities, with particular emphasis on the near-bed velocity, were introduced. The results presented were consistent with Section 4.1.

Table 3 presents the percentage reduction in the maximum scour depth and length due to baffle piers with different angles relative to the smooth apron. The table confirmed the findings in Fig. 12(a), in which the maximum reductions in scour depth and length were observed for Pθ = 45 °. On the contrary, the minimum reductions in scour length and width were observed for the apron with baffle piers oriented toward the flow direction (Pθ = 135 °).

Fig. 12(b) was plotted to investigate the effect of baffle pier height, P_h, on the bed topography. The figure was presented for a constant Q = 40 L/s, Pθ = 45 °, and yt = 18 cm. The figure showed similar behavior across the bed configurations, in which the local scour depth decreased as the baffle pier height increased. The increase in baffle pier height caused the installed baffle piers to face the greater jet flow beneath the sluice gate. Consequently, greater dissipation of jump energy and a smaller effect on the bed material. These findings were consistent with Fig. 7(b). The figure shows that the maximum local scour depth decreased by 74.87%, 78.07%, and 83.96% for Ph = 6cm, 9cm, and 12cm, respectively. Additionally, the presence of baffle piers, regardless of height, resulted in approximately a 41.54% reduction in scour length relative to the smooth apron.

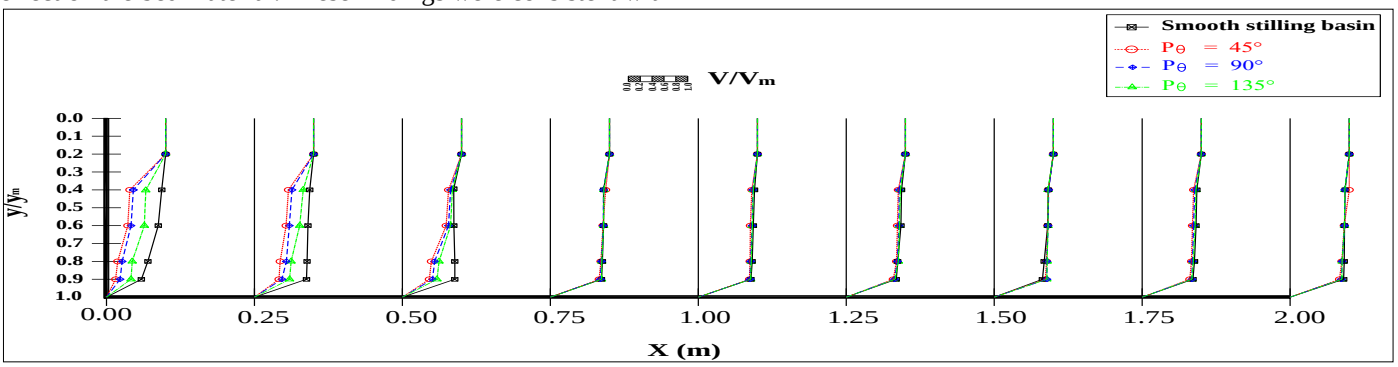

Figure 9. Vertical velocity distributions at different sections along the flume length downstream the stilling basin toe, Q= 40 Lit/s, y_t= 18 cm, and P_h= 12 cm.

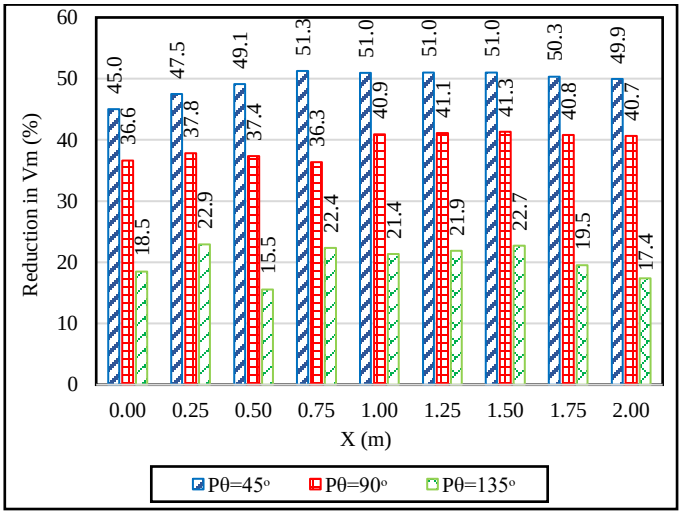

Figure 10. Percentages of reduction in V_m, for different P_θ, along the flume length, at Q= 40 Lit/s, y_t= 18 cm, and P_h= 12 cm.

Table 3. Reduction in maximum local scour geometry

P_θ	% Reduction in maximum local scour	
	Depth	Length
45°	297.87	56.82
90°	163.38	38.01
135°	40.60	23.21

5. Conclusions

This research experimentally investigated the influence of installing baffle piers on a stilling basin apron downstream of a sluice gate. The study evaluated the performance of various baffle pier heights and angles under different flow conditions and compared the results to a smooth apron reference case.

The primary findings of this study are as follows:

- The installation of bottom baffle piers significantly improves hydraulic performance compared to a smooth apron. The optimal configuration was identified as 12 cm-high baffle piers angled at 45° to the flow.
- This optimal design effectively controlled the hydraulic jump, decreasing its dimensionless length by approximately 45-47% and increasing energy dissipation efficiency by roughly 46-60%. The maximum velocity was also reduced by nearly 33%.
- Baffle piers were highly effective at minimizing downstream scour. The analysis showed that scour depth decreased as the baffle pier height increased and the angle of inclination decreased.
- From a practical standpoint, the optimal apron design offers a clear advantage for real-world applications. By allowing for shorter, more efficient stilling basins, this configuration can significantly reduce construction costs. This provides a tangible benefit for engineering projects, particularly in irrigation systems where budgets are often constrained.

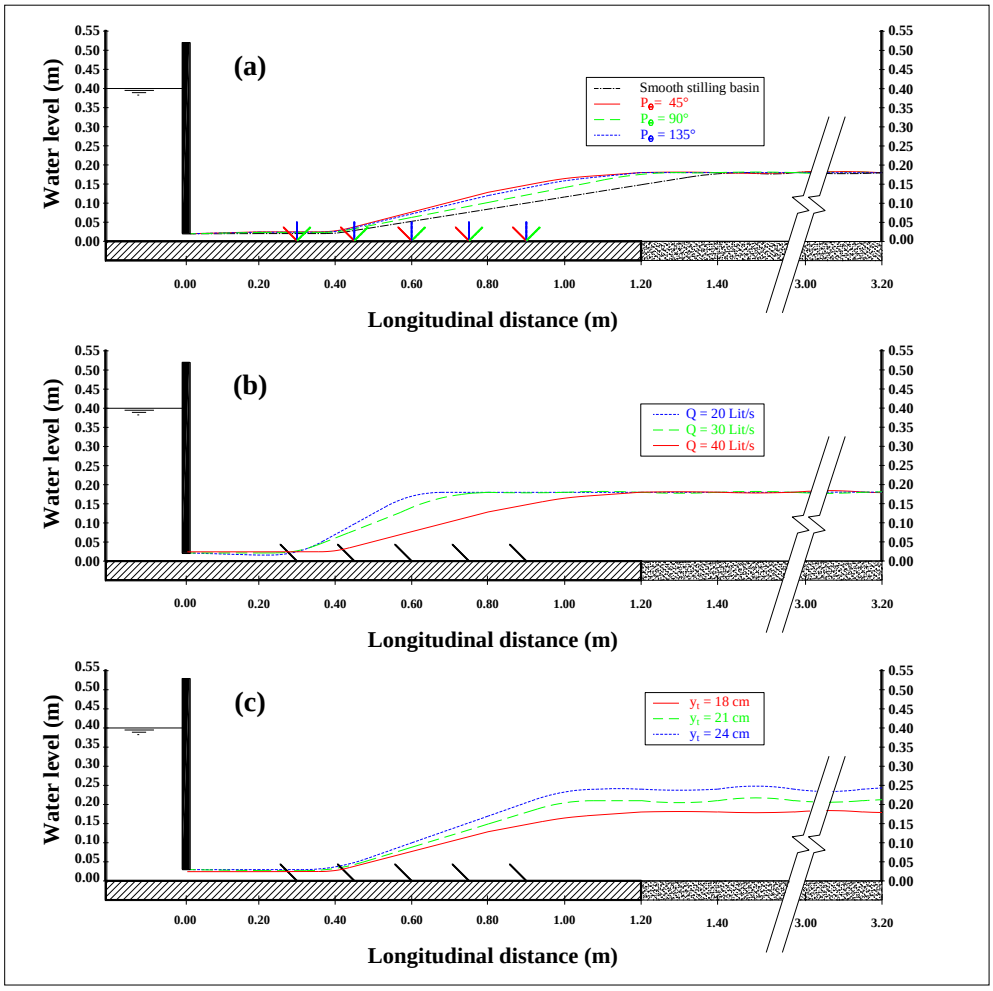

Figure 11. Water surface profiles for (a) different P_θ at Q=40 Lit/s and y_t =18 cm; (b) different Q at P_θ = 45° and y_t =18 cm; (c) different y_t at Q=40 Lit/s and P_θ = 45°

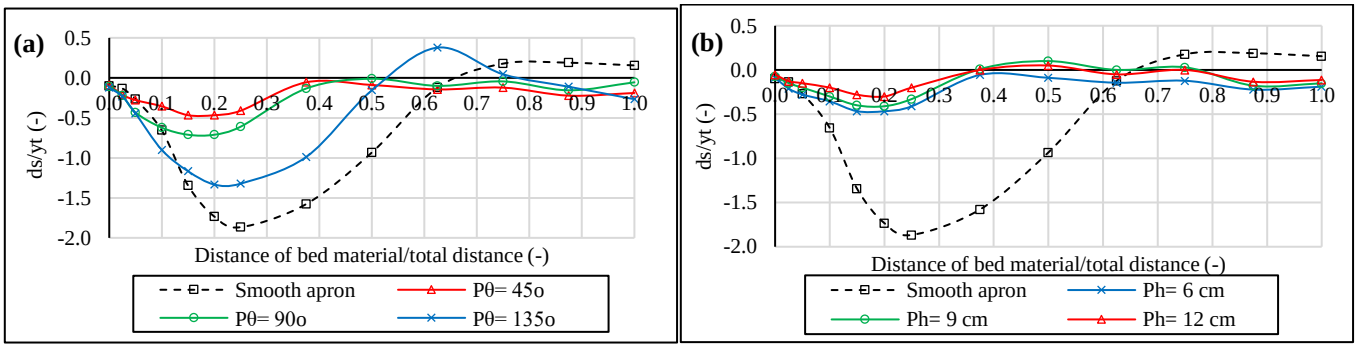

Figure 12. Effect of the baffle piers on the bed configurations for different: (a) P_θ; (b) P_h.

.

Conflict of Interest

The authors declare that there are no conflicts of interest regarding the publication of this manuscript.

Author Contribution Statement

Ibrahim M.M. and Ahmed M. Ibraheem proposed the research problem. Ibrahim M.M., Baydaa Hamdi Salih, and Ahmed M. Ibraheem developed the theory and performed the computations. Ibrahim M.M., Abeer Samy, and Ahmed M. Ibraheem verified the analytical methods and supervised the findings of this work. All authors discussed the results and contributed to the final manuscript.

Acknowledgements

This work was conducted at the Hydraulics Research Institute, National Water Research Center, Egypt. The authors are

grateful for the valuable collaboration and efforts of all Institute staff members.

Abbreviations

B	Flume width [m]
d_{50}	Median particle diameter [mm]
d_s	Maximum scour depth [cm]
E_1	Initial specific energy [m]
E_2	Sequent specific energy [m]
g	Gravity acceleration [m/s^2]
H_{up}	The upstream water head [cm]
L_f	Stilling basin length [m]
L_j	hydraulic jump length [cm]
L_s	Maximum scour length [cm]
P_d	Baffle pier distance from the sluice gate [m]
P_h	Baffle pier height [cm]
P_w	Baffle pier width [cm]
P_θ	Baffle pier angle concerning flow direction.
Q	Flow discharge [degree]
S_o	Flume bed slope [Lit/s]
V	Mean longitudinal velocity [m/s]
V_1	Hydraulic jump initial velocity [m/s]
V_2	Hydraulic jump sequent velocity [m/s]
V_m	Maximum velocity at any cross-section downstream of the apron [m/s]
X	Longitudinal distance measured from the stilling basin toe [m]
y	Flow depth at a given point [cm]
y_1	Hydraulic jump initial flow depth [cm]
y_2	Hydraulic jump sequent flow depth [cm]
y_g	Gate opening [cm]
y_t	Tailwater depth [cm]
ρ	Water density of the flow [kg/m^3]
ρ_s	Soil particle density [kg/m^3]
γ_b	Bulk unit weight [gm/cm^3]
μ	Water dynamic viscosity [kg/m.s]
σ	Water surface tension [N/m]
σ_g	Geometric standard deviation
η	Energy dissipation efficiency
R_e	Reynolds number
F_r	Froude number
W_e	Weber number

References

[1] M. C. Aydin and A. E. Ulu, "Effects of Different Shaped Baffle Blocks on the Energy Dissipation and the Downstream Scour of a Regulator," *Bitlis Eren University Journal of Science and Technology*, vol. 8, no. 2, pp. 69–74, Dec. 2018, doi: https://doi.org/10.17678/beuscitech.469053

[2] A. Q. Rdhaiwi, A. Khoshfetrat, and A. Fathi, "Experimental Investigation of Scour Downstream Of A C-Type Trapezoidal Piano Key Weir With Stilling Basin," *Journal of Engineering and Sustainable Development*, vol. 27, no. 6, pp. 688–697, Nov. 2023, doi: https://doi.org/10.31272/jeasd.27.6.2

[3] F. Fatima, M. K. Sarwar, F. U. Haq, and A. Raza, "CFD Simulation of hydraulic jump in the USBR type-III stilling basin with converged walls," *AQUA — Water Infrastructure, Ecosystems and Society*, vol. 73, no. 5, pp. 888–901, May 2024, doi: https://doi.org/10.2166/aqua.2024.317.

[4] Y. K. Abdelmonem, S. Shabayek, and A. O. Khairy, "Energy dissipation downstream sluice gate using a pendulum sill," *Alexandria Engineering Journal*, vol. 57, no. 4, pp. 3977–3983, Dec. 2018, doi: https://doi.org/10.1016/j.aej.2018.01.019.

[5] M. A. Ashour, T. Sayed, and S. El-Attar, "Impact of Curved Shaped Energy Dissipaters Downstream of Head Structures on Both Water Energy Dissipation and Irrigation Water Quality," *Limnological Review*, vol. 15, no. 1, pp. 3–14, Mar. 2015, doi: https://doi.org/10.2478/limre-2015-0001

[6] H. Abdel Samad, Y. E. Helal, S. A. Ibrahim, and M. F. Sobeih, "Minimizing Scour Downstream Hydraulic Structures Using Semi–Circular Sill," *ERJ. Engineering Research Journal*, vol. 35, no. 2, pp. 129–137, Apr. 2012, doi: https://doi.org/10.21608/erjm.2012.67127

[7] P. Fošumpaur, T. Kašpar, M. Králík, and M. Zukal, "Study of Boundary Conditions for Design of New Types of Fibre Concrete Energy Dissipators in Hydraulic Structures," *IOP Conference Series: Materials Science and Engineering*, vol. 596, no. 1, p. 012031, Aug. 2019, doi: https://doi.org/10.1088/1757-899x/596/1/012031.

[8] R. Daneshfaraz, S. Sadeghfam, and A. Tahni, "Experimental Investigation of Screen as Energy Dissipators in the Movable-Bed Channel," *Iranian Journal of Science and Technology Transactions of Civil Engineering*, vol. 44, no. 4, pp. 1237–1246, Sep. 2019, doi: https://doi.org/10.1007/s40996-019-00306-7.

[9] A. Abbas, H. Alwash, and A. Mahmood, "Effect of baffle block configurations on characteristics of hydraulic jump in adverse stilling basins," *MATEC Web of Conferences*, vol. 162, p. 03005, May 2018, doi: https://doi.org/10.1051/matecconf/201816203005

[10] E. A. Elnikhely, "Investigation and analysis of scour downstream of a spillway," *Ain Shams Engineering Journal*, vol. 9, no. 4, pp. 2275–2282, Dec. 2018, doi: https://doi.org/10.1016/j.asej.2017.03.008.

[11] M. M. Ibrahim, "Effect of Angled Submerged Vanes on Bed Morphology Downstream Sluice Gate," *Journal of Scientific Research and Reports*, vol. 22, no. 4, pp. 1–16, Mar. 2019, doi: https://doi.org/10.9734/jsrr/2019/v22i430094

[12] H. Dashtban, A. Kabiri-Samani, M. Fazeli, and M. Rezashahreza, "Hydraulic jump in a circular stilling basin by using angled baffle blocks," *Flow Measurement and Instrumentation*, vol. 96, p. 102562, Apr. 2024, doi: https://doi.org/10.1016/j.flowmeasinst.2024.102562.

[13] M. Aamir, Z. Ahmad, M. Pandey, M. A. Khan, A. Aldrees, and A. Mohamed, "The Effect of Rough Rigid Apron on Scour Downstream of Sluice Gates," *Water (Basel)*, vol. 14, no. 14, p. 2223, Jul. 2022, doi: https://doi.org/10.3390/w14142223.

[14] S. H. Hojjati and A. R. Zarrati, "Numerical Study of Scouring Downstream of a Stilling Basin," Environmental Fluid Mechanics, vol. 21, no. 2, pp. 465–482, Feb. 2021, doi: https://doi.org/10.1007/s10652-021-09781-x.

[15] E. Helal, "Minimizing scour downstream of hydraulic structures using single line of floor water jets," *Ain Shams Engineering Journal*, vol. 5, no. 1, pp. 17–28, Mar. 2014, doi: https://doi.org/10.1016/j.asej.2013.06.001.

[16] A. M. A. Amin, "Physical model study for mitigating local scour downstream of clear over-fall weirs," *Ain Shams Engineering Journal*, vol. 6, no. 4, pp. 1143–1150, Dec. 2015, doi: https://doi.org/10.1016/j.asej.2015.03.013.

[17] E. Helal, F. S. Abdelhaleem, and W. A. Elshenawy, "Numerical Assessment of the Performance of Bed Water Jets in Submerged Hydraulic Jumps," *Journal of Irrigation and Drainage Engineering*, vol. 146, no. 7, Jul. 2020, doi: https://doi.org/10.1061/(ASCE)IR.1943-4774.0001475

[18] S. Erryanto and V. Dermawan, "Double sill stilling basin to enhance energy dissipation for a strong hydraulic jump with a high Froude number," *IOP Conference Series: Earth and Environmental Science*, vol. 1311, no. 1, p. 012009, Mar. 2024, doi: https://doi.org/10.1088/1755-1315/1311/1/012009.

[19] O. K. Saleh, E. A. Elnikhely, and F. Ismail, "Minimizing the hydraulic side effects of weirs construction by using labyrinth weirs," *Flow Measurement and Instrumentation*, vol. 66, pp. 1–11, Apr. 2019, doi: https://doi.org/10.1016/j.flowmeasinst.2019.01.016.

[20] M. C. Tuna and M. E. Emiroglu, "Scour profiles at downstream of cascades," *Scientia Iranica*, vol. 18, no. 3, pp. 338–347, Jun. 2011, doi: https://doi.org/10.1016/j.scient.2011.05.040.

[21] T. R. Al-Husseini, H. T. Hamad, and A.-S. T. Al-Madhhachi, "Effects of an Upstream Sluice Gate and Holes in Pooled Step Cascade Weirs on Energy Dissipation," *International Journal of Civil Engineering*, vol. 19, no. 1, pp. 103–114, Sep. 2020, doi: https://doi.org/10.1007/s40999-020-00568-7

[22] S. S. Muhsun, A.-S. T. Al-Madhhachi, and Z. T. Al-Sharify, "Prediction and CFD Simulation of the Flow over a Curved Crump Weir under Different Longitudinal Slopes," *International Journal of Civil Engineering*, vol. 18, no. 9, pp. 1067–1076, Jun. 2020, doi: https://doi.org/10.1007/s40999-020-00527-2

[23] T. R. Al-Husseini, A.-S. T. Al-Madhhachi, and Z. A. Naser, "Laboratory Experiments and Numerical Model of Local Scour around Submerged Sharp Crested Weirs," *Journal of King Saud University - Engineering Sciences*, vol. 32, no. 3, pp. 167–176, Mar. 2020, doi: https://doi.org/10.1016/j.jksues.2019.01.001

[24] C. Fang, "Open-Channel Flows," *Springer Textbooks in Earth Sciences, Geography and Environment*, pp. 437–453, Dec. 2018, doi: https://doi.org/10.1007/978-3-319-91821-1_10.